Dosimetry Contribution:

Evaluation of a novel software application for magnetic resonance distortion correction in cranial stereotactic radiosurgery

Juan-Francisco Calvo-Ortega, MSc,*,† José Mateos, PhD,‡ Ángel Alberich, PhD,§
Sandra Moragues, RTT,*,† Juan-José Acebes, PhD,* and Joan Casals, MD*,†

*Servicio de Oncología Radioterápica, Hospital Quirónsalud, Barcelona, Spain; †Servicio de Oncología Radioterápica, Hospital Universitari Dexeus, Barcelona, Spain; ‡Imagen Ensayos Clínicos (IEC), Hospital Quirónsalud, Barcelona, Spain; and §Biomedical Imaging Research Group (GIBI230), La Fe Health Research Institute, Valencia, Spain

ABSTRACT

This study aimed to validate a novel commercially available software for correcting spatial distortion in cranial magnetic resonance (MR) images. This software has been used to assess the dosimetric impact of MR distortion in stereotactic radiosurgery (SRS) treatments of vestibular schwannomas (VSs). Five MR datasets were intentionally distorted. Each distorted MR dataset was corrected using the Cranial Distortion software, obtaining a new corrected MR dataset (MRcorr). The accuracy of the correction was quantified by calculating the target registration error (TRE) for 6 anatomical landmarks identified in the co-registered MRcorr and planning computed tomography (pCT) images. Nine VS cases were included to investigate the impact of the MR distortion in SRS plans. Each SRS plan was calculated on the pCT ($1 \times 1 \times 1$ mm³ voxel) with the target and organs at risk (OARs) delineated using the planning MR dataset. This MR dataset was then corrected (MRcorr) using the Cranial Distortion software. Geometrical agreement between the original target and the corresponding corrected target was assessed using several metrics: MacDonald criteria, mean distance to agreement (MDA), and Dice similarity coefficient (DSC). Target coverage (D99%) and maximum doses (D2%) to ipsilateral cochlea and brainstem resulting on the MRcorr dataset were compared with the original values. TRE values (0.6 mm ± 0.3 mm) and differences found in Macdonald criteria (0.3 mm ± 0.4 mm and 0.3 mm ± 0.3 mm) and MDA (0.8 mm ± 0.2 mm) were mostly within the voxel size dimension of the pCT scan ($1 \times 1 \times 1$ mm³). High similarity (DSC > 0.7) between the original and corrected targets was found. Small dose differences for the original and corrected structures were found: 0.1 Gy ± 0.1 Gy for target D99%, 0.2 Gy ± 0.3 Gy for cochlea D2%, and 0.1 Gy ± 0.1 Gy for brainstem D2%. Our study shows that Distortion Correction software can be a helpful tool to detect and adequately correct brain MR distortions. However, a negligible dosimetric impact of MR distortion has been detected in our clinical practice.

© 2018 American Association of Medical Dosimetrists.

Introduction

Stereotactic radiosurgery (SRS) is a well-established technique to treat surgically inaccessible lesions within the brain.[1] The use of magnetic resonance (MR) imaging is required to perform SRS because of its superiority over computed tomography (CT) in soft tissue contrast and sensitivity for delineating targets and normal brain tissue.[2] However, stereotactic MR imaging is more susceptible than CT to spatial distortion that may lead to targeting errors.[3]

System-related and patient-induced geometric distortions have been described for MR imaging. The first type of distortion is generated mainly by magnet inhomogeneities and nonlinearity of the gradient fields.[4] Main MR imaging vendors have incorporated postprocessing algorithms to correct the system-related distortion, reducing the geometrical error down to 2 mm.[5] Siebert *et al.*[6] have described that the gradient nonlinearity causes distortion in MR imaging that can displace intracranial targets by nearly 4 mm, with a potential displacement up to 8 mm. They concluded that, although MR imaging distortion is often subtle on visual inspection, there is a significant clinical impact of this distortion on SRS planning. Siebert *et al.* considered a significant clinical impact ("missed target") caused by the MR distortion if more than 10% of the true gross target volume receives less than 90% of the prescription dose (*i.e.*, V90 < 90%) or if the underdosed (< 90% of prescription) portion of the true gross target volume was greater than 125 mm^3.

Patient-induced geometric distortions are due to the phenomenon named chemical shift[7] and susceptibility differences between tissues.[8] Magnetic susceptibility-induced distortion is typically smaller than system-related distortion but still non-negligible, with maximum distortion ranging from 2.1 to 2.6 mm at a field strength of 1.5 Tesla (T).[9] Kondziolka *et al.*[10] reported that magnetic susceptibility artifacts may produce anatomical distortions larger than 2 mm, resulting in inaccurate stereotactic target localization. Targeting errors, especially in lesions that abut air spaces such as the internal auditory canal, have been reported in the literature.[11] Pollock *et al.*[12] reported that distortion of stereotactic MR imaging may cause that some vestibular schwannomas (VSs) receive less than the prescribed radiation dose to the entire tumor volume.

In this study, we investigate the accuracy of a recently released software designed to correct spatial distortions of MR images used for cranial SRS planning. We also assess the dosimetric impact of the MR imaging distortion in SRS plans computed in our department.

Methods and Materials

Patients to be treated with cranial SRS in our department are immobilized using a thermoplastic mask. The planning CT (pCT) scan is acquired (Somaton, Siemens Medical Systems, Erlangen, Germany) without intravenous contrast, with 125 kV, 686 mAs, 1-mm slice thickness, 500-mm field of view, and matrix of 512 × 512 pixels, that is, 1 mm reconstructed in plane resolution.

Patient MR imaging is acquired (without the mask) using a 1.5 T scanner (Siemens Symphony, Siemens Medical Systems). A three-dimensional postgadolinium T1-weighted MPRAGE (magnetization-prepared rapid acquisition with gradient echo) sequence was acquired: TE 3.26 milliseconds, TR 1950 milliseconds, flip angle of 15°, and voxel spacing 1 × 1 × 1 mm^3. The automated distortion correction protocol provided by the MR scanner was used during acquisition. Planning MR (pMR) is obtained with an axial reconstruction at 1-mm slice intervals for SRS planning (250-mm field of view and 512 × 512 matrix, *i.e.*, 0.5-mm pixel size).

Evaluation of MR-related geometric distortion

A dedicated phantom supplied by the manufacturer (Brainlab AG, Munich, Germany) was used to measure the system-related geometric distortion. The phantom consists of a plastic parallelepiped (135 × 120 × 170 mm^3) containing a pattern of 21 cubes (1-cm side) on its "right" plate and another pattern of 15 cubes (1-cm side) on the "feet" side (Fig. 1A). It was filled with water for MR imaging. After delicate positioning of the phantom at the center of the head coil, it was MR imaged using the SRS patient protocol described earlier. The 1-cm side cube patterns located at the "right" and "feet" sides of the phantom can be visualized in the corresponding sagittal and axial slices, respectively (Fig. 1B). The magnitude of distortion was evaluated by measuring the cube sides and by comparing with the known side length (1 cm) as certified by Brainlab. Measurements were performed in the 3 anatomical planes (axial, sagittal, and coronal) using the Brainlab iPlan RT Image 4.1 software.

Validation of Brainlab software to correct MR distortion

As noted previously, distortion-corrected MR imaging should uniformly be used for intracranial SRS planning because uncorrected MR images can lead to potential geometric miss.[6] The manufacturer Brainlab has developed the Elements Cranial Distortion Correction application to correct distortions in MR images. Henceforth, this software will be referred to as "Distortion Correction." Distortion Correction uses a deformable MR-CT co-registration, creating an additional corrected MR dataset (MRcorr) while keeping the original structures that are deformed according to the MR distortion magnitude (Fig. 2). The corrected structures are also mapped to the pCT, in such a way that 2 structure sets
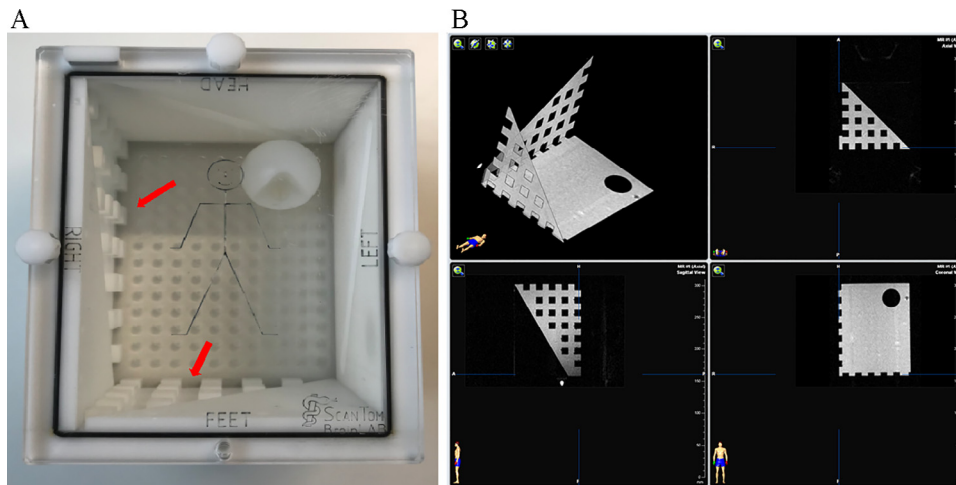
A   B

Fig. 1. (A) Brainlab phantom: red arrows show the 1-cm cube patterns used. (B) Sagittal and axial MR planes through the "right" and "feet" plates of the phantom, respectively. (Color version of figure is available online.)
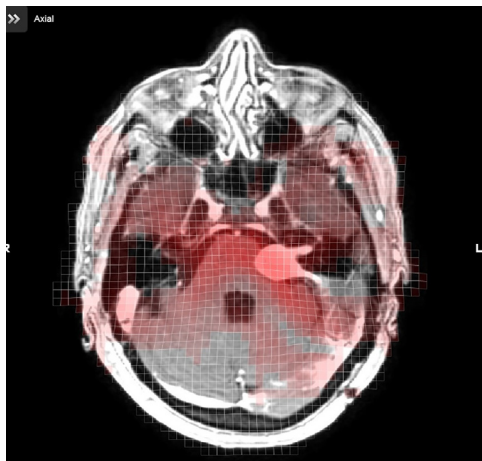

Fig. 2. Example of distortion map displayed by the Distortion Correction application after correcting an MR dataset. Graphically, distortion correction magnitude is illustrated with a grid. (Color version of figure is available online.)

are present on the pCT scan (original and corrected structures, Fig. 3). The pCT dataset is considered as the reference image space. The algorithm is described in a technical note reported by Brainlab[13]: for cranial SRS planning, the algorithm automatically identifies the fusion scenario MR/CT and subsequently defines a scenario-specific image subvolume. Afterward, this subvolume is further subdivided into $(3 \times 3 \times 3)$ cm³ overlapping window patches. Based on an initial rigid fusion between the fused datasets, affine patch-wise registrations are performed for every three-dimensional patch to locally align the imaged anatomies and thus to account for local mismatches. Subsequently, the local registrations are interpolated to generate a single, continuous deformation field that maps one of the datasets onto the other, while bringing the local correspondences to a match. Reliable fusion is accomplished by an outlier detection applied to the patch-wise fusions.
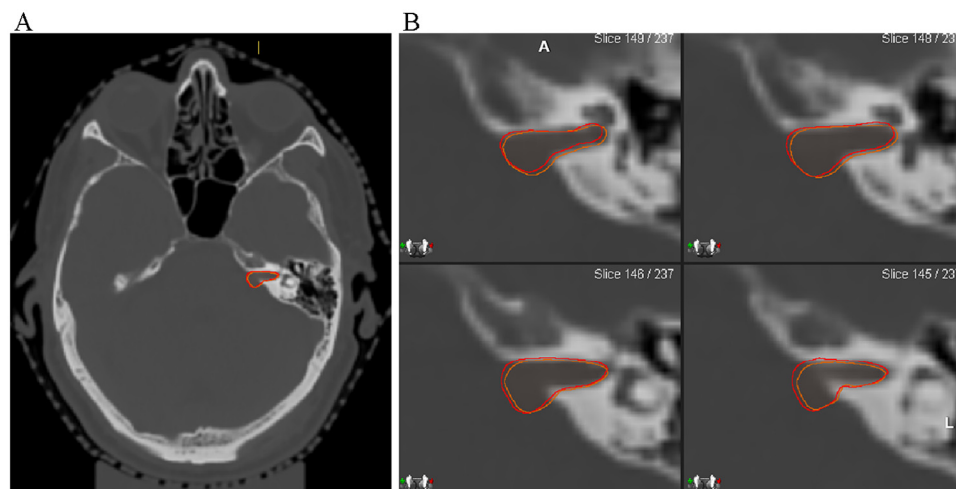
A   B

Fig. 3. (A) Original VS target (red contour) and its MR distortion-based correction (orange contour) mapped onto the planning CT. (B) Axial, sagittal, and coronal views are shown after image zooming from the target area. (Color version of figure is available online.)

According to the Brainlab technical white paper,[13] the approach used by Cranial Distortion Correction is based on a patented Brainlab Synthetic Tissue Model and MR imaging sequence detection. Besides MR scanner-specific correction methods, as far as we know, this is the only commercially available product that enables retrospective correction for geometric distortions in MR imaging, so far. So, we consider that Cranial Distortion Correction is a "novel" application.

To investigate the accuracy of the Distortion Correction application, an evaluation was performed on 5 patient data. For each case, the original MR (MRorig) dataset used for SRS planning was artificially distorted (MRdist) using Matlab R2016a (MathWorks Inc., Natick, MA). Two types of distortions, emulating distortion artifacts as the ones produced by severe gradient failures, were applied:

$$s = r\left(1 + 0.1\,r^2\right), \text{ denoted as "dist1"} \qquad (1)$$

$$s = r\left(1 + 0.5\,r\right), \text{ denoted as "dist2"} \qquad (2)$$

where s and r are the distances from the center of distortion in the distorted and undistorted images, respectively. Maximum spatial distortions of 3 and 5 mm were forced with dist1 and dist2, respectively. Distortion larger than 5 mm ("dist3") was also induced by replacing the factor 0.1 by 0.5 in Eq. (1), but immediately we observed that Distortion

Correction was not able to correct this large distortion. Errors larger than 5 mm are unlikely to happen in the clinical practice for cranial SRS. Weygand *et al.*[9] did a bibliographic review of the geometric distortion in MR imaging-guided radiotherapy (not specifically focused on cranial SRS). Eleven studies reported phantom measurements quantifying system-dependent geometric distortion. Although distortion errors on the centimeter scale were reported, the majority of the distortions were less than 5 mm. In fact, errors larger than 5 mm were observed at large distances from the scanner isocenter (> 95 mm), that is, distortion errors larger than 5 mm are unlikely to happen for cranial SRS cases. Also, 2 studies cited by Weygand *et al.*[9] reported susceptibility-induced distortions less than 3 mm at a field strength of 1.5 T.

In contrast, MR distortions greater than 5 mm have not been detected in our SRS clinical practice so far. For instance, a large distortion (> 5 mm) during planning of a VS radiosurgery would be easily detectable after CT/MR registration in our treatment planning system by checking the anatomical coincidence using the internal auditory canal. Obviously, an MR scan with a distortion greater than 5 mm must be rejected for targeting in radiosurgery. So, our study was just focused on distortions within 5 mm as represented by Eqs. (1) and (2). Figure 4 shows an example of the MRorig set and its corresponding MRdist sets for a VS case.

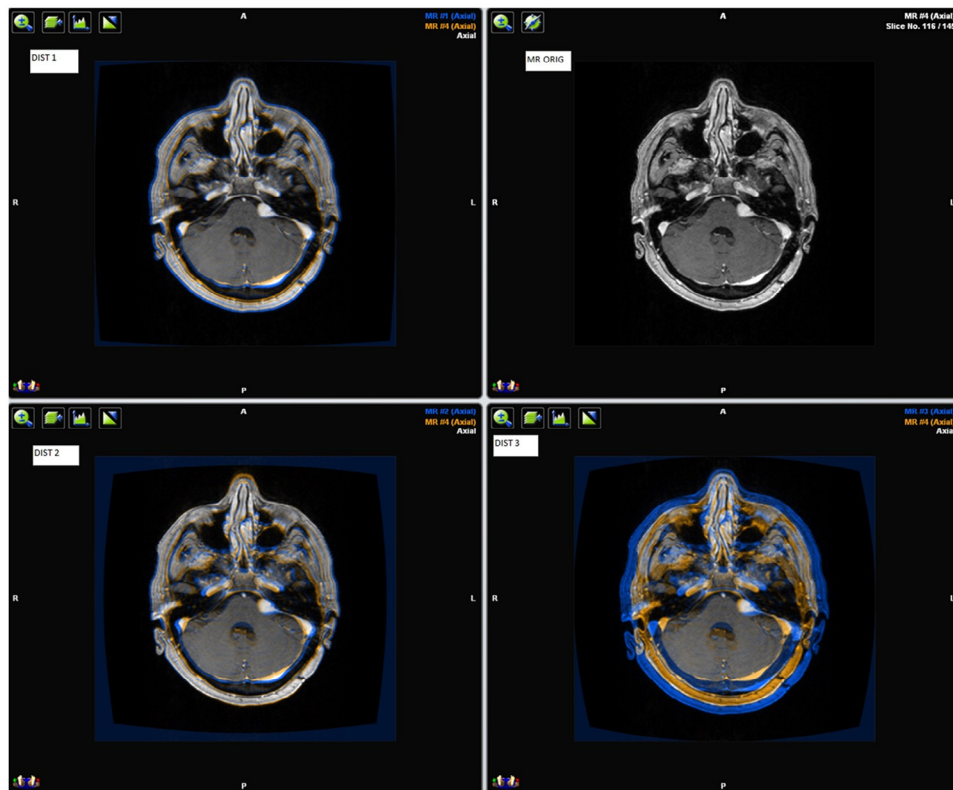**Fig. 4.** Example of distortions forced to an original MR dataset (upper right). Upper left: distorted MR using "dist1" blended with the original MR set; bottom left: distorted MR using "dist2" blended with the original MR set; bottom left: distorted MR using "dist3" blended with the original MR set. Orange: original MR set; blue: distorted MR set. (Color version of figure is available online.)

For each patient case, the MRdist dataset was corrected using the Distortion Correction application, generating a corrected MR dataset (MRcorr). The MRcorr and the MRorig images were each one rigidly co-registered to the pCT scan using the Brainlab iPlan RT Image 4.1 software (pCT/MRcorr and pCT/MRorig, respectively). In contrast, the MRorig/MRdist pair was automatically fused because both datasets shared the same DICOM frame of reference. Therefore, the MRdist dataset was directly co-registered with the pCT scan via 2 registration pairs: MRorig/MRdist and pCT/MRorig.

Several anatomically recognizable landmarks were selected in the pCT image space using a point tool available on Brainlab iPlan RT Image 4.1 software. These points were selected again in the corresponding co-registered MRcorr, MRdist, and MRorig datasets. The chosen landmarks were points of the 2 vestibules, internal auditory canals and cochleas, as they were easy to identify in pCT and MR images. One well-trained observer (neurosurgeon) identified the positions of these landmarks in 2 separate passes (Fig. 5). According to AAPM TG-132 task group report,[14] interobserver variation is typically larger than intraobserver variability, so having the same observer to identify the same landmark on both images will reduce the uncertainty in the localization. Each landmark was selected in 2 different slices in both co-registered datasets (pCT and MR). CT is generally assumed not to need distortion correction in contrast to MR imaging.[4,15-17] It was also confirmed by the monthly checks on the CT scanner used in this study. Therefore, the pCT dataset was selected in this study as the reference image (ground truth) to specify the "true" position of each selected landmark.

The pCT/MR registration accuracy can be assessed by measuring the Euclidian distance between the paired landmarks identified for each anatomical structure on both image modalities. This distance is often referred to as the target registration error (TRE).[18] From now on, the TRE metric is denoted in this study as "TREcorr" and "TREdist" when pCT/MRcorr and pCT/MRdist registrations are evaluated, respectively. TREcorr gives the accuracy of the Distortion Correction application for correction of distorted MR images, whereas TREdist indicates the magnitude of the intended distortion. The task was performed twice by the observer in different days to consider intraobserver variability, and the average values of TREcorr and TREdist were reported in this study.

Dosimetric impact of MR distortion

Nine VS patients were enrolled in this study. The pCT and MRorig images acquired for the treatment planning of each patient were retrieved and imported in the Brainlab Elements software. Both image sets were registered using the Elements Image Fusion application (release 3.0.0.60), using a rigid fusion algorithm based on mutual information. Then, the target was automatically delineated using the Elements SmartBrush application (release 2.5.0.131), whereas the organs at risk (OARs) brainstem and ipsilateral cochlea were automatically segmented using the Elements Anatomical Mapping application (release 1.0.0.77). All delineated structures were revised by a radiation oncologist and adapted as required. A structure dataset ("original structures") is available on the pCT scan after being mapped from the MRorig dataset. After that, the potential distortion associated to the MRorig dataset was corrected using the Distortion Correction application (release 3.0.0.60).

Three metrics were used to assess the impact of MR geometric distortion on the target structure:

(1) The Macdonald criteria[19] were computed for each paired target (original and corrected) mapped on the pCT dataset. The Elements SmartBrush application includes an algorithm to compute the Macdonald criteria for the target. It is defined as the product

Fig. 5. Anatomical landmarks (red crosses; C: cochlea, IAC: internal auditory canal, and V: vestibule). Right image was zoomed from the left image. (Color version of figure is available online.)
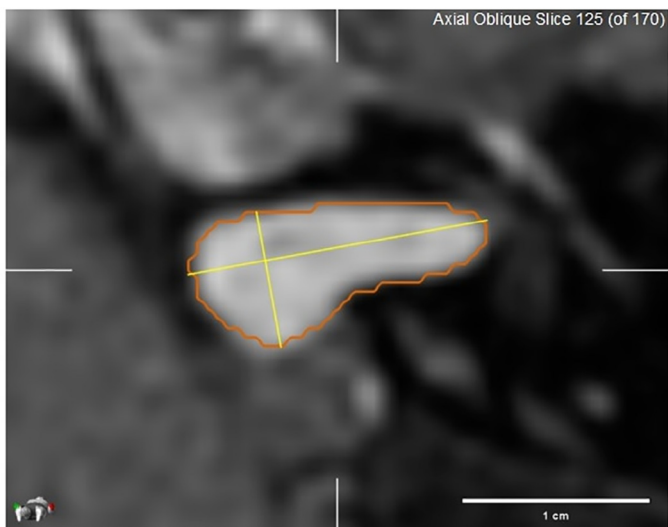
Fig. 6. Example of Macdonald criteria computed by Elements SmartBrush application. (Color version of figure is available online.)

of the longest diameter (L) within all CT slices and the longest perpendicular diameter (P) within the slice where the longest diameter has been detected (Fig. 6).

(2) The maximum separation distances between the original and the corrected targets were manually measured in the axial, sagittal, and coronal CT slices for each VS case (Fig. 7). The average of these 3 distances was considered an estimation of mean distance to agreement (MDA).[20]

(3) The agreement between original and corrected targets was assessed using the Dice similarity coefficient (DSC).[21] DSC is defined as 2 times the volume where the 2 delineated structures overlap divided by the total volume of both structures combined. As the structures approach agreement, the DSC value approaches 1; as the volumes diverge into 2 nonoverlapping structures, the DSC value goes to 0. A DSC value < 0.7 is considered an indicator of low similarity.[22]

The following pass/fail values for the Macdonald, MDA, and DSC metrics were established in our work: 1 mm (corresponding to the voxel size of the pCT) for the Macdonald and MDA metrics,[14] whereas a tolerance of 0.7 was established for the DSC metric.[22]

For each patient, a SRS reference plan was calculated over the pCT scan using the Eclipse treatment planning system (version 13.7, Varian Medical Systems, Palo Alto, CA). The reference plan consisted of 15 noncoplanar
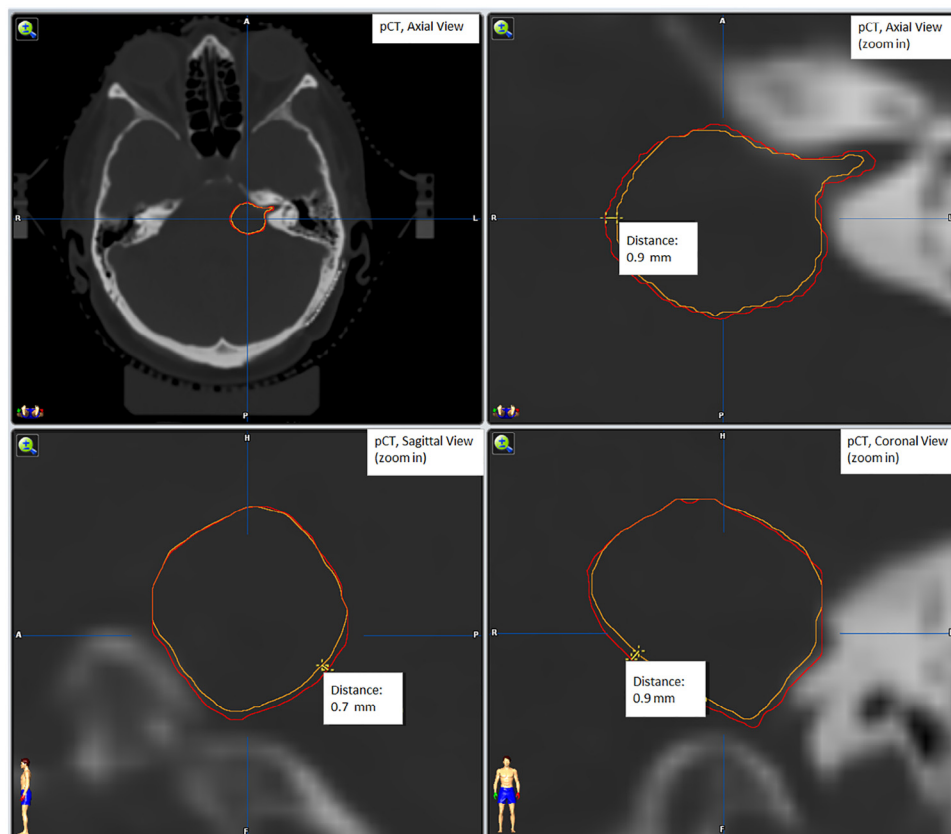

Fig. 7. Example of distances between targets (red: original; orange: corrected) manually measured in the 3 anatomical planes. Axial, sagittal, and coronal views are shown after image zooming from the target area. (Color version of figure is available online.)

intensity-modulated (IMRT) fields of 6 MV from a Varian linac.[23] IMRT dose-based inverse optimization was performed considering the original structures. The dose calculation was done using the Anisotropic Analytical Algorithm of the Eclipse, with a calculation grid size of 1 mm. For SRS planning, larger grid sizes are not recommended as small lesions are treated with small fields and high calculated dose accuracy is required.[24] The reference plan was optimized to achieve target coverage and dose constraints for the OARs (brainstem and ipsilateral cochlea). After that, the doses to all corrected structures were retrieved to investigate the dosimetric impact of not using the cranial distortion correction. Maximum doses (D2%) to ipsilateral cochlea and brainstem, as well as the target coverage (D99%), were analyzed, where Dx% is the minimum dose to x% of the volume.

Results

MR geometric distortion measurements using the Brainlab phantom were 0.3 mm ± 0.2 mm, 0.6 mm ± 0.3 mm, and 0.5 mm ± 0.2 mm in the axial, sagittal, and coronal planes, respectively. A maximum distortion of 1.3 mm was found in the sagittal plane, whereas a tolerance of 1.5 mm was recommended by Brainlab when their dedicated phantom is used.

Figure 8 shows the target registration errors (TREcorr and TREdist) between the paired landmarks identified on the pCT, MRcorr, and MRdist datasets for the 2 kinds of forced distortions applied in this study. Average values of TREcorr over the 5 cases were always within the pCT voxel size ($1 \times 1 \times 1$ mm³). A clear improvement in the CT/MR agreement was found when the Distortion Correction software was used: TREcorr = 0.6 mm ± 0.2 mm *vs*

TREdist = 1.7 mm ± 0.7 mm; for dist1; and TREcorr = 0.6 mm ± 0.4 mm *vs* TREdist = 2.0 mm ± 1.4 mm; for dist2. Irrespective of the type of distortion applied, TREcorr = 0.6 mm ± 0.3 mm *vs* TREdist = 1.9 mm ± 1.1 mm. According to our data, the Distortion Correction application was able to correct at most 5-mm distortions induced on MR images.

Table 1 shows the differences in the metrics Macdonald criteria, MDA, and DSC between the targets initially delineated on the MRorig datasets and the corrected ones that were generated after applying the Distortion Correction application. In general, the differences found on Macdonald criteria and MDA were within the pCT voxel size ($1 \times 1 \times 1$ mm³). High values of similarity (DSC > 0.7) were found between the original and corrected targets in all VS cases analyzed. Small dose differences were found between the original and corrected structures: 0.1 Gy ± 0.1 Gy for target D99% [values of D99%: 12.4 Gy ± 0.3 Gy *vs* 12.4 Gy ± 0.3 Gy], 0.2 Gy ± 0.3 Gy for cochlea D2% [values of D2%: 9.0 Gy ± 3.0 Gy vs. 9.2 Gy ± 3.0 Gy], and 0.1 Gy ± 0.1 Gy for brainstem D2% [values of D2%: 5.5 Gy ± 3.1 Gy *vs* 5.6 Gy ± 3.2 Gy]. Therefore, the dosimetric impact of MR distortion was negligible in real VS cases treated in our department.

Discussion

This study was mainly focused on a geometric analysis to evaluate the performance of the Distortion Correction software. According to our measurements using the Brainlab phantom, the MR scanner-related distortion was within the 1 mm³ voxel size used in our cranial SRS protocol. Therefore, the distortion correction procedure provided with the MR scanner used in this study was capable of minimizing the magnitude of the system-related distortion, at least
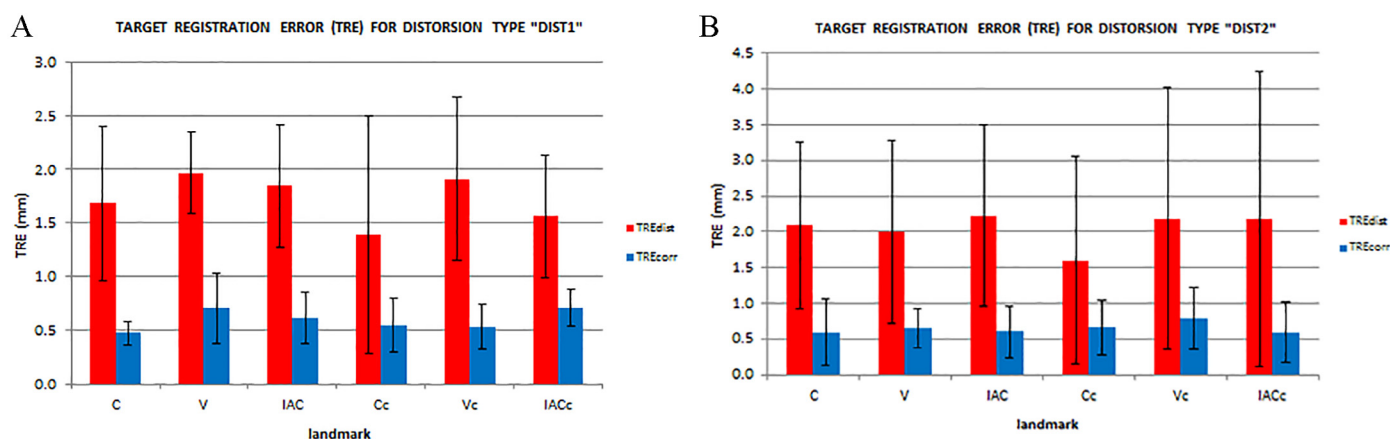
Fig. 8. Target registration errors (TREs) of five MR datasets (mean and standard deviation) using 6 anatomical landmarks for the distortions "dist1" (A) and "dist2" (B). Red columns: average TRE between the distorted MR set and the planning CT (TREdist). Blue columns: average TRE between the corrected MR set and the planning CT (TREcorr). Standard deviation is displayed as a bar on each column. C, ipsilateral cochlea; V, ipsilateral vestibule; IAC, ipsilateral internal acoustic canal; Cc, contralateral cochlea; Vc, contralateral vestibule; IACc, contralateral internal acoustic canal. (Color version of figure is available online.)

Table 1
Differences found on the metrics used to assess the geometrical and dosimetric agreement between structures defined in the original MR dataset and the corresponding corrected structures after distortion correction

No. of VS case	L-Macdonald[a] (mm)	P-Macdonald[b] (mm)	MDA (mm)	DSC	D99% (Gy) target[c]	D2% (Gy) ipsilateral cochlea[d]	D2% (Gy) Brainstem[d]
1	0.5	0.8	0.4	0.94	0.1	0.0	0.0
2	1.3	0.4	0.9	0.95	0.1	0.0	0.3
3	0.3	0.3	0.7	0.92	0.0	0.0	0.0
4	0.2	0.1	0.8	0.91	0.4	0.0	0.0
5	0.0	0.0	0.8	0.89	0.0	0.0	0.1
6	0.1	0.2	1.1	0.87	0.1	0.3	0.0
7	0.1	0.2	0.8	0.94	0.1	0.8	0.0
8	0.0	0.5	0.9	0.87	0.0	0.3	0.2
9	0.1	0.00	0.6	0.93	0.1	0.8	0.0
Mean	**0.3**	**0.3**	**0.8**	**0.91**	**0.1**	**0.2**	**0.1**
SD	**0.4**	**0.3**	**0.2**	**0.03**	**0.1**	**0.3**	**0.1**

SD, standard deviation.

[a] L-Macdonald is the longest diameter (L) within all CT slices.

[b] P-Macdonald is the longest perpendicular diameter (P) within the CT slice where the longest diameter has been detected.

[c] D99% is the minimum dose received by the 99% of the target volume.

[d] D2% is minimum dose to the 2% of volume.

for the scanning range used in our cranial SRS protocol ($256 \times 256 \times 145$ mm³). However, patient-induced distortions are not considered for correction by the MR scanner manufacturer procedures. Some procedures have been described to correct the distortion caused by the susceptibility difference in the human brain near interfaces between air or bone and brain tissues.[25,26] Also, techniques that allow correcting chemical shift effects have been presented in the literature,[27,28] but none of these correction techniques are available in our department.

The commercially available Distortion Correction software is a promising tool developed to overcome the MR distortions produced by the patient and the MR scanner. In this study, we have performed the validation of this software using intentionally distorted MR sets, with distortion magnitude up to 5 mm. In general, the Distortion Correction software was able to reduce the distortion within the 1 mm³ voxel size used in our clinical images. As far as we know, the only validation to date of the Distortion Correction software has been performed by Brainlab.[13] The 2 anterior brain ventricular horns were chosen as anatomical landmarks to measure the TRE distances over CT/MR fused datasets of 37 patients. Cranial Distortion revealed accuracy (TREcorr) of 1.3 mm ± 1.2 mm, whereas a value of 0.6 mm ± 0.3 mm for TREcorr was found in our study. Differences in these TRE values were obviously due to the different procedures used by Brainlab and the one used in our study. MR datasets used in the Brainlab validation were not intentionally forced to have a large distortion (~5 mm); therefore, our validation procedure consisted of a more demanding scenario to check the performance of the Distortion Correction software.

Our study was limited to 2 types of intended distortions (dist1 and dist2), forcing distortions up to 5 mm. To

stress the Correction Distortion, a more extreme distortion equation was also applied (dist3). It was created by replacing the factor 0.1 by 0.5 in the equation of dist1 to increase the magnitude of the distortion beyond 5 mm. However, Distortion Correction was not able to give a solution below 1 mm, as it is illustrated in Fig. 9: the intracanalicular component of the VS lesion, as seen on the corrected MR images, did not match with the corresponding area on the CT scan. However, errors larger than 5 mm are unlikely to happen in the clinical practice of cranial SRS as long as the patient's head is placed at the center of the MR imaging bore. Siebert *et al.*[6] published their experience about MR distortion in cranial SRS. They observed distortions less than 5 mm when
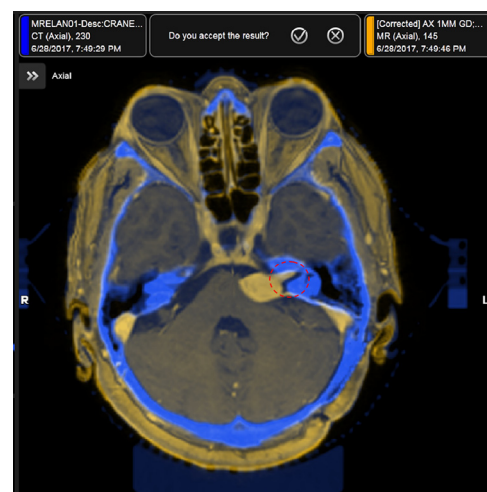

Fig. 9. Example of corrected MR set after applying the distortion type "dist3." Orange: corrected MR set; blue: planning CT set. Red dotted circle shows a clear mismatching in the intracanalicular zone for a right-sided VS. (Color version of figure is available online.)

the patient's head was centrally placed in the scanner bore that is the typical patient setup used in our department during MR imaging for cranial SRS planning.

The chemical shift and other artifacts were not specifically included in our validation of the Distortion Correction software. For instance, the chemical shift has been previously demonstrated to introduce additional geometric errors of up to 1.5 mm.[29] We think that the distortions used in our study (dist1 and dist2) are covering a wide clinical range (up to 5 mm) and different scenarios of potential MR distortion errors.

Some practical limitations of the Distortion Correction software were detected during our study: (1) this software does not provide a quantitative report (*e.g.*, in terms of TRE or DSC values) analyzing the agreement between the resulting MR corrected and the CT scan (ground truth). In a clinical use, the accuracy of the correction performed by the software relies only on the observer visual inspection of the images. (2) The use of phantoms (real or virtual) with unambiguous landmarks or known deformations may be very helpful to check the accuracy of the Distortion Correction software. However, this software does not support the use of phantoms.

Once the Distortion Correction software was validated, we proceeded to analyze the dosimetric impact of the potential MR distortions for 9 VS cases previously treated in our department. The pMR datasets were corrected by applying the Distortion Correction software. Doses to the corrected structures (targets and OARs) were retrieved from the SRS plans that were designed using the pMR without distortion correction and which were registered with the pCT. As shown in Table 1, the potential MR distortions (scanner-related and patient-induced) did not produce major dosimetric differences even for very highly conformal IMRT plans. Obviously, these results could not be attained without an adequate tuning of the MR scanner. For instance, Siebert *et al.*[6] described how no-corrected gradient fields led to inadequate dose coverage of the true target with subdosage up to 75% (*i.e.*, 75% of target volume received less than 90% of the prescribed dose). The true target was considered to be missed in the Siebert's study if more than 10% of the volume receives less than 90% of the prescription. No missing target was observed in our study.

According to our results (Table 1), the pMR datasets acquired in our clinical practice were adequate for planning cranial VS SRS treatments without the need to be corrected using the Distortion Correction software. In our department, there is not a dedicated quality assurance program focused on SRS planning to assess the accuracy of the MR scanners. Even when an MR scanner demonstrates compliance with the measurements described by the American Association of Physicists in Medicine (AAPM), meaningful distortion may still be present.[5] An AAPM report in 2005

warned about the verification of whether the stereotactic software used is able to detect and correct MR distortions, as not all commercially available SRS platforms have these capabilities.[30] Definitively, we think that the use of a distortion correction tool as the one presented in this study is highly recommended when SRS of small cranial lesions is practiced. To our knowledge, this is the first independent study to assess the use of the Distortion Correction software in cranial SRS plans. Accuracy of the Distortion Correction software was validated using intended distortions up to 5 mm, but errors of this magnitude and larger are unlikely to arise in the clinical practice. Our study was limited to the use of a 1.5 T MR scanner and only VS cases were investigated. Further investigation will be needed in the future to consider these limitations.

Conclusions

Geometric displacements caused by MR distortions were less than 1 mm in the target vicinity for real VS cases treated in our department. Although a negligible dosimetric impact caused by MR distortion was observed in our clinical VS cases, the Distortion Correction software was proved in our study as a helpful tool to detect and adequately correct brain MR distortions.

References

1. Leksell, L. The stereotaxic method and radiosurgery of the brain. *Acta Chir. Scand.* **102**(4):316–9; 1951.
2. Sze, G.; Milano, E.; Johnson, C.; *et al.* Detection of brain metastases: Comparison of contrast-enhanced MR with unenhanced MR and enhanced CT. *AJNR Am. J. Neuroradiol.* **11**(4):785–91; 1990.
3. Condon, B.; Hadley, D. Errors in MR stereotaxy due to undetected extraneous metal objects. *Phys. Med. Biol.* **42**(9):1779–89; 1997.
4. Baldwin, L.N.; Wachowicz, K.; Thomas, S.D.; *et al.* Characterization, prediction, and correction of geometric distortion in 3 T MR images. *Med. Phys.* **34**(2):388–99; 2007.
5. Wang, D.; Strugnell, W.; Cowin, G.; *et al.* Geometric distortion in clinical MRI systems. Part II: Correction using a 3D phantom. *Magn. Reson. Imaging* **22**(9):1223–32; 2004.
6. Seibert, T.M.; White, N.S.; Kim, G.Y.; *et al.* Distortion inherent to magnetic resonance imaging can lead to geometric miss in radiosurgery planning. *Pract. Radiat. Oncol.* **6**(6):e319–28; 2016.
7. Smith, A.S.; Weinstein, M.A.; Hurst, G.C.; *et al.* Intracranial chemical-shift artifacts on MR images of the brain: Observations and relation to sampling bandwidth. *AJR Am. J. Roentgenol.* **154**(6):1275–83; 1990.
8. Schenck, J.F. The role of magnetic susceptibility in magnetic resonance imaging: MRI magnetic compatibility of the first and second kinds. *Med. Phys.* **23**(6):815–50; 1996.

9. Weygand, J.; Fuller, C.D.; Ibbott, G.S.; *et al*. Spatial precision in magnetic resonance imaging-guided radiation therapy: The role of geometric distortion. *Int. J. Radiat. Oncol. Biol. Phys.* **95**(4):1304–16; 2016.

10. Kondziolka, D.; Dempsey, P.K.; Lunsford, L.D.; *et al*. A comparison between magnetic resonance imaging and computed tomography for stereotactic coordinate determination. *Neurosurgery* **30**(3):402–6; 1992, discussion 406–7.

11. Jezzard, P.; Balaban, R.S. Correction for geometric distortion in echo planar images from B0 field variations. *Magn. Reson. Med.* **34**(1):65–73; 1995.

12. Pollock, B.E.; Link, M.J.; Foote, R.L. Failure rate of contemporary low-dose radiosurgical technique for vestibular schwannoma. *J. Neurosurg.* **111**(4):840–4; 2009.

13. Cranial Distortion Correction. Technical background. Available at: https://www.researchgate.net/publication/317359164. Accessed May 9, 2017.

14. Brock, K.K.; Mutic, S.; McNutt, T.R.; *et al*. Use of image registration and fusion algorithms and techniques in radiotherapy: Report of the AAPM Radiation Therapy Committee Task Group No. 132. *Med. Phys.* **44**(7):e43–76; 2017.

15. Curry, T.S.; Dowdey, J.E.; Murry, R.C. Christensen's Physics of Diagnostic Radiology. Philadelphia: Lea & Febiger; 1990.

16. Price, R.G.; Knight, R.A.; Hwang, K.P.; *et al*. Optimization of a novel large field of view distortion phantom for MR-only treatment planning. *J. Appl. Clin. Med. Phys.* **18**(4):51–61; 2017.

17. Torfeh, T.; Hammoud, R.; Perkins, G.; *et al*. Characterization of 3D geometric distortion of magnetic resonance imaging scanners commissioned for radiation therapy planning. *Magn. Reson. Imaging* **34**(5):645–53; 2016.

18. Fitzpatrick, J.M.; West, J.B.; Maurer, C.R. Jr. Predicting error in rigid-body point-based registration. *IEEE Trans. Med. Imaging* **17**(5):694–702; 1998.

19. Macdonald, D.R.; Cascino, T.L.; Schold, S.C. Jr; *et al*. Response criteria for phase II studies of supratentorial malignant glioma. *J. Clin. Oncol.* **8**(7):1277–80; 1990.

20. Chalana, V.; Kim, Y. A methodology for evaluation of boundary detection algorithms on medical images. *IEEE Trans. Med. Imaging* **16**(5):642–52; 1997.

21. Dice, L.R. Measures of the amount of ecologic association between species. *Ecology* **26**:297–302; 1945.

22. Zijdenbos, A.P.; Dawant, B.M.; Margolin, R.A.; *et al*. Morphometric analysis of white matter lesions in MR images: Method and validation. *IEEE Trans. Med. Imaging* **13**(4):716–24; 1994.

23. Calvo-Ortega, J.F.; Delgado, D.; Moragues, S.; *et al*. Dosimetric comparison of intensity modulated radiosurgery with dynamic conformal arc radiosurgery for small cranial lesions. *J. Cancer Res. Ther.* **12**(2):852–7; 2016.

24. Ong, C.L.1.; Cuijpers, J.P.; Senan, S.; *et al*. Impact of the calculation resolution of AAA for small fields and RapidArc treatment plans. *Med. Phys.* **38**(8):4471–9; 2011.

25. Holland, D.; Kuperman, J.M.; Dale, A.M. Efficient correction of inhomogeneous static magnetic field-induced distortion in Echo Planar Imaging. *Neuroimage* **50**(1):175–83; 2010.

26. Weis, J.; Ericsson, A.; Silander, H.C.; *et al*. Magnetic resonance spectroscopic imaging for visualization and correction of distortions in MRI: High precision applications in neurosurgery. *Magn. Reson. Imaging* **16**(10):1265–72; 1998.

27. Chang, H.; Fitzpatrick, J.M. A technique for accurate magnetic resonance imaging in the presence of field inhomogeneities. *IEEE Trans. Med. Imaging* **11**(3):319–29; 1992.

28. Cho, Z.H.; Kim, D.J.; Kim, Y.K. Total inhomogeity correction including chemical shifts and susceptibility by view angle tilting. *Med. Phys.* **15**(1):7–11; 1988.

29. Mack, A.; Wolff, R.; Scheib, S.; *et al*. Analyzing 3-tesla magnetic resonance imaging units for implementation in radiosurgery. *J. Neurosurg.* **102**(suppl.):158–64; 2005.

30. Lightstone, A.W.; Benedict, S.H.; Bova, F.J.; *et al*. Intracranial stereotactic positioning systems: Report of the American Association of Physicists in Medicine Radiation Therapy Committee Task Group no. 68. *Med. Phys.* **32**(7):2380–98; 2005.